

1 **Oceanographic features delineate growth zonation in Northeast Pacific**
2 **sablefish**

3
4 Kapur, M.¹, Haltuch, M.², Connors, B.³, Rogers, L.⁴, Berger, A.², Koontz, E.⁵, Cope, J.², Echave,
5 K.⁶, Fenske, K.⁶, Hanselman, D.⁶, Punt, A.E.¹

6
7 ¹University of Washington, School of Aquatic and Fisheries Sciences. 1122 NE Boat St, Seattle WA 98105

8 ²Fisheries Resource and Monitoring Division, Northwest Fisheries Science Center, National Marine Fisheries Service
9 National Oceanic and Atmospheric Administration. 2725 Montlake Blvd. E. Seattle, WA 98112

10 ³Institute of Ocean Sciences, Fisheries and Oceans Canada. 9860 W. Saanich Rd. Sidney, B.C. Canada V8L 5T5

11 ⁴Fisheries and Oceans Canada, School of Resource and Environmental Management, Simon Fraser University. 8888
12 University Drive, Burnaby, British Columbia, Canada, V5A 1S6

13 ⁵Center for Quantitative Science, Ocean Teaching Building, Suite 300, Box 357941, Seattle, WA 98195.

14 ⁶Auke Bay Laboratories, Alaska Fisheries Science Center, National Marine Fisheries Service National Oceanic and
15 Atmospheric Administration. 17101 Pt. Lena Loop Rd. Juneau, AK 99801

16
17 Corresponding author: kapurm@uw.edu

18
19 Keywords: growth, von Bertalanffy, ecosystem-based fisheries management, sablefish,
20 spatiotemporal

21
22 **Abstract**

23 Renewed interest in the estimation of spatial and temporal variation in fish traits, such as body
24 size, is a result of computing advances and the development of spatially-explicit management
25 frameworks. However, many attempts to quantify spatial structure or the distribution of traits
26 utilize *a priori* approaches, which involve pre-designated geographic regions and thus cannot
27 detect unanticipated spatial patterns. We developed a new, **model-based** method that uses the first
28 derivative of the spatial smoothing term of a generalized additive model to identify spatial zones
29 of variation in fish length-at-age. We use simulation testing to evaluate the method across a variety
30 of synthetic, stratified age and length datasets, and then apply it to survey data for Northeast Pacific
31 sablefish (*Anoplopoma fimbria*). Simulation testing illustrates the robustness of the method across
32 a variety of scenarios related to spatially or temporally stratified length-at-age data, including strict
33 boundaries, overlapping zones and changes at the extreme of the range. Results indicate that
34 length-at-age for Northeast Pacific sablefish increases with latitude, which is consistent with
35 previous work from the western United States. Model-detected spatial breakpoints corresponded
36 to major oceanographic features, including the northern end of the Southern California Bight and
37 the bifurcation of the North Pacific Current. This method has the potential to improve detection of
38 large-scale patterns in fish growth, and aid in the development of spatiotemporally structured
39 population dynamics models to inform ecosystem-based fisheries management.

40 **1 Introduction**

41 There is no consensus on how to model region-specific growth patterns in assessment or
42 population dynamics models. Fish somatic growth rates are typically modelled using the von
43 Bertalanffy growth function (VBGF, von Bertalanffy, 1957) or an alternative functional form, with
44 parameters estimated using model-fitting procedures. The spatial resolution of the resultant
45 estimates is necessarily predicated on the aggregation of the data, which is often defined by survey
46 stratification, political or management boundaries, and/or changes in sampling gear, not
47 necessarily the ecology of the population (McGarvey and Fowler, 2002; Williams et al., 2012).
48 For example, assessments of Alaskan sablefish stocks estimated separate VBGF parameters for
49 two periods of survey data based on the *a priori* hypothesis that changes in survey gear type would
50 affect estimates of fish growth from survey data (Echave et al., 2012; Hanselman et al., 2017;
51 McDevitt, 1990), and imposed a time block between which estimates of the growth curve
52 parameters were quite similar in the stock assessment (

53 Table 1). More sophisticated approaches that utilize hierarchical Bayesian methods to estimate
54 latitudinal and regional effects on length- or weight-at-age require a design matrix of dimensions
55 dictated by pre-supposed zones (e.g. Adams et al., 2018). Such approaches are useful within a
56 management context with rigid spatial boundaries, but do not represent the underlying growth
57 process explicitly, and preclude the discovery of spatially-structured trends in fish size that do not
58 match current management boundaries.

59 Existing methods to quantify spatial variation in somatic growth pose a trade-off. On one hand,
60 researchers may impose *a priori* beliefs about spatial variation in stock traits or generate purely
61 descriptive models of trait ‘gradients’ across regions or time periods, without a clear way to
62 identify significant break points within them (King et al., 2001). This presents a challenge when
63 developing population dynamics models that accurately represent the structure of managed stocks.
64 An alternative tool is a model-based method that identifies break points in fish size-at-age, which
65 can then be used to aggregate data and estimate parameters related to somatic growth. The
66 significance of these breaks can be evaluated by comparing overlap in growth parameter estimates
67 and tested against or among pre-specified breaks of interest (i.e. an area with a known ecosystem
68 regime). To meet this need we present a new method, which uses the first derivative of smooth
69 functions (splines) from a generalized additive model (GAM) to detect change points in spatially-
70 and temporally-structured fisheries growth data that minimizes the use of pre-supposed
71 stratifications in a simple, rapid computational framework. The method does not require the
72 specification of multiple error structures nor the construction of spatial meshes, which can be
73 computationally expensive when large (Thorson, 2019). The analysis of first derivatives of
74 regression splines in GAMs for change-point analysis has been recently used in terrestrial
75 paleoecology (Simpson, 2018) and geophysics (Beck et al., 2018). The underlying assumption is
76 that the rate of change (the first derivative) of a given predictor is an appropriate measure of the
77 direction and magnitude of the predictor-response relationship. The spline itself may be highly

78 non-linear, but predictor values at which the slope of the spline is largely positive or negative are
79 taken to denote where the response variable is changing the most.

80 Our **GAM-based** method has the potential to improve detection of large-scale patterns in fish
81 growth, and aid in the development of spatially-structured population dynamics models. We use
82 simulation to test the robustness of the method using synthetic length-at-age data of varied
83 complexity, and present a case study application to Northeast Pacific sablefish (*Anoplopoma*
84 *fimbria*). Sablefish are a highly mobile, long-lived, and valuable groundfish that have high
85 movement rates (10 – 88% annual movement probabilities across Alaska, with a mean great-circle
86 distance of 191 km in a single year; Hanselman et al. 2015) and range from Southern California to
87 the Bering Sea. Concurrent population declines across the entire range over the past few decades
88 have increased concern about the status of sablefish, and interest in identifying the causes of the
89 downward trend. **Sablefish stock assessment and management occur independently within political**
90 **boundaries**, namely Alaska (AK), British Columbia (BC), and the US West Coast in the California
91 Current (CC), assuming that these are closed stocks. However, recent work has shown that there
92 is little genetic evidence for population differentiation in sablefish across the NE Pacific
93 (Jasonowicz et al., 2017), although there is evidence for differences in growth rate and size-at-
94 maturity throughout the range (McDevitt, 1990). This suggests that the current delineation of
95 assessment and **management areas** may be incongruent with the stock's actual spatial structure and
96 underscores the potential value of developing a population dynamics model that represents the
97 heterogeneity of sablefish growth throughout their range.

98 We developed a data-model-based method that would simultaneously identify spatiotemporal
99 zones between which fish length-at-age varies and illustrate correlations between growth and
100 spatiotemporal covariates (such as an increase with latitude). A method to identify such patterns
101 in important population traits can help researchers determine whether current management scales
102 are appropriate given the dynamics present in the population. Because these dynamics are
103 potentially environmentally linked, such a method can also uncover whether spatiotemporal
104 patterns in investigated traits correspond to major environmental features (such as ocean currents)
105 or forcings (such as climactic oscillations), which can help inform the implementation of
106 ecosystem-based fisheries management.

107 **2 Methods**

108 *2.1 Method summary*

109 The method fits a GAM to the vector of observed lengths of fish of a single age as the response
110 variable, predicted by separate smoothers at knots t for year, latitude, and longitude, using the
111 mgev package (Wood, 2011) in R (R Development Core Team, 2016), i.e.

112
$$\text{Equation 1 } g(\mathbf{E}(\mathbf{X})) = \beta_0 + f(y_t) + f(s_t) + f(k_t) + \epsilon_t$$

113 where $\mathbf{E}(\mathbf{X})$ represents the expected mean of fish length, g is an invertible, monotonic link function
114 (in this case, the natural logarithm) that enables mapping from the response scale to the scale of
115 the linear predictor, and the additive effects of latitude (s_t), longitude (k_t) and year (y_t), which are
116 smoothed using a thin plate regression spline f . ϵ_t is a residual error term assumed to be normally

117 distributed. The effects of latitude, longitude and year on expected length-at-age are estimated as
 118 separate smoothers. To simplify the analysis, we fit the GAM to data for a single age-class and sex
 119 at once (e.g., age six for the simulated datasets), thus precluding the need to control for age or sex.
 120 Using fish of only a single selected age from all regions also minimizes the concern of differing
 121 age-based survey selectivities between management areas.

122 The first derivatives of the linear predictor with respect to latitude, longitude and year are
 123 evaluated to identify areas or periods (breakpoints) between which there is evidence for changes
 124 in fish length-at-age. The equations below provide an example using latitude s_t , but the process is
 125 repeated for each smoother. The finite differences method (as in Simpson, 2018) approximates the
 126 first derivative of the trend from the fitted GAM. For instance, the vector of derivatives \mathbf{G} for
 127 latitude is produced via the following:

128 Equation 2 $\mathbf{G}_t = \frac{g(s_t + \alpha) - g(s_t)}{\alpha}$

129 where $g(S_t)$ is a vector of predicted fish lengths at latitudes and $\alpha = 0.001$ in this analysis, with
 130 other effects (year, longitude) held constant. Therefore, the numerators of the elements of \mathbf{G} are
 131 predicted lengths at two adjacent latitudes, separated by interval α , which is necessarily small.

132 The standard error of the derivative estimates are computed as:

133 Equation 3 $SE_t = \sqrt{\mathbf{G}_t \mathbf{V}}$

134 where \mathbf{V} is the variance for the current spline; the square root provides the standard error for each
 135 derivative estimate of that predictor. These steps are repeated across the range of explored years
 136 and longitudes. All simulated datasets (Section 2.2.1) were fit using a link function g with
 137 smoothing functions f for both spatial covariates as well as for year. For each parameter, we
 138 identify at which predictor value (e.g., latitude) the maximum absolute value of the first derivative
 139 is obtained; this is rounded to the nearest integer (e.g. a value between 22.5 and 23.4 would be
 140 rounded to 23) and defined as the “breakpoint” if its 95% confidence interval (generated using the
 141 standard error estimates for the derivative) does not include zero (see Figure 1 and 2, which
 142 illustrate the raw data, smoothers and first derivatives thereof for two synthetic datasets). The
 143 rounding step was implemented to ease comparison in the simulation study; we did not wish to
 144 treat a breakpoint estimate as incorrect if it differed by less than half of one degree (approximately
 145 55 kilometers) from the true breakpoint. The raw length and age data (including all ages of fish)
 146 are then re-aggregated based on the identified breakpoints. For each of these new aggregated data
 147 sets, the parameters of the VGBF (Equation 4; L_∞ - asymptotic length [cm], k - the rate at which
 148 asymptotic length is approached [cm/yr] and t_0 - the estimated age at length zero in years) are
 149 estimated using maximum likelihood, assuming that errors are normally distributed with zero mean
 150 and standard deviation σ). This study performed estimation using Template Model Builder
 151 (Kristensen et al., 2016).

152 Equation 4 $\bar{L}_a = L_\infty \times (1 - \exp(-k(a - t_0))) + \varepsilon ; \quad \varepsilon \sim N(0, \sigma^2)$

153 2.2 *Simulation testing*

154 2.2.1 Outline and design

155 We conducted a simulation study to evaluate the performance of the proposed GAM-based
 156 method, based on datasets generated using an individual-based model (IBM, see Supplementary
 157 Material for full details). The IBM is capable of simulating individual characteristics by following
 158 the life history processes (survival and growth) of individual fish, with reproduction governed by
 159 a generalized stock-recruitment relationship to produce new individuals. An IBM was used to
 160 capture these key processes to simulate data similar in form to what would be included in a fishery
 161 stock assessment, which is difficult to do analytically or using age/size aggregated models. We
 162 simulate spatial variation by generating length-at-age datasets under different growth ‘Regimes’
 163 (defined as distinct L_1 and/or L_2 values, leading to varied L_∞) and assign latitudes and longitudes
 164 to fish grown under each regime. The IBM implements the VBGF using Schnute’s (1981)
 165 formulation, which requires k , L_1 , and L_2 , with L_∞ computed as:

166 Equation 5 $L_\infty = L_1 + \frac{L_2 - L_1}{1 - e^{-k(a_2 - a_1)}}$

167 where L_1, L_2 represent the expected lengths of fish at ages a_1, a_2 , (3 and 30 years, respectively)
 168 and k is the growth coefficient. Each annual increment for every individual fish is subject to
 169 lognormal error. We considered five growth scenarios consisting of two growth “Regimes” with
 170 either completely distinct spatial or temporal ranges, or spatial ranges with some overlap. We
 171 designed our growth regimes to mimic the level of variation in L_1 and L_2 present in the sablefish
 172 dataset, which was as high as 26%. In our synthetic population for regime 1 $L_1 = 10$ cm, $L_2 = 70$
 173 cm and $k = 0.30$ yr⁻¹; regime 2 was designed using L_1 and L_2 parameters 20% higher than regime
 174 1 ($L_1 = 12$ cm, and $L_2 = 84$ cm, $k = 0.30$ yr⁻¹). Expected growth curves for the simulated Regimes
 175 are present in Supplementary Figure A2.

176 The simulated spatial extent ranges from 0° to 50° in latitude and longitude. The five
 177 simulation scenarios (Table 2) were designed to represent a variety of possibilities for spatial
 178 growth variation, with one scenario including a temporal regime change in growth. To simulate
 179 spatial zones, locations of fish grown under a certain regime were sampled from a uniform
 180 distribution with boundaries defined by the spatio-temporal scenario at hand (Figure 3). All fish in
 181 scenario 1 (no spatial or temporal variation) were grown under regime 1 and sampled (uniformly)
 182 over latitude and longitude between 0° to 50°. In scenario 2, fish were grown in two regimes, and
 183 fish grown under regime 1 were between 0° and 25° (latitude and longitude) while fish grown
 184 under regime 2 had coordinates sampled between 25° to 50°. The same approach was applied for
 185 scenario 3, except that fish grown under regime 2 were sampled from 20° to 50°, thus creating an
 186 overlap zone between 20° and 25°. All simulated fish in scenario 4, had latitudes sampled from
 187 0° to 50°. Fish simulated under regime 1 were assigned longitudes sampled randomly from 0° to
 188 48° and fish simulated under regime 2 have longitudes sampled randomly from 48° to 50°, forming
 189 a vertical “band” of larger fish in higher longitudes.

190 The final simulation scenario (5) involved temporal changes in growth, with a change from
 191 growth regime 1 to regime 2 in year 50. This meant that the growth increment generally increased

192 for individuals whose lifespan covers this breakpoint, though note that the GAM is fit to fish of a
193 fixed age. Fish locations for the temporal break scenario are sampled identically to the scenario
194 without spatial variation.

195 Under each scenario, 100 replicate datasets were generated, which averaged 530 age-six fish
196 per dataset (a sensitivity analysis was performed reducing the sample size by 25% or 50%). For
197 all runs, the initial values for the parameters were $t_0 = 0.1$ yrs, $\sigma = 1.1$, with $L_\infty = 150$ cm and $k =$
198 0.1. The estimation procedure also calculated the predicted length at the endpoints of the estimated
199 growth curve (Equation 5; the length at pre-specified minimum (L_1) and maximum (L_2) ages,
200 which were 3 and 30 years in the simulation studies). These values and their standard errors were
201 used in the evaluation of the method (see Section 2.2.2 Performance metrics), as L_∞ and k are
202 typically negatively correlated.
203

204 2.2.2 Performance metrics

205 We considered two performance metrics: 1) the proportion of simulations in which the correct
206 spatial and/or temporal breakpoints were detected - we tabulated the number of times a breakpoint
207 found using a GAM fit to a dataset matched the true latitude, longitude, and year; and 2) the
208 coverage probabilities (determined by the 95% confidence intervals) for L_1 and L_2 . For all but the
209 scenario with overlapping ranges (scenario 3), we only considered the GAM analysis to have
210 correctly identified the true breakpoint only if it was an exact match. The ‘true’ dataset for scenario
211 3 contained fish grown under regimes 1 and 2 in a shared region between 20° and 25° latitude and
212 longitude, so the detected breakpoint was counted as an accurate match if it fell within this range.
213

214 For each scenario, after aggregating each of the 100 simulated datasets into the GAM-
215 designated spatiotemporal strata and estimating the growth curve, we determined whether the 95%
216 confidence intervals of the estimated fish lengths at ages zero and fifteen (our a_1 and a_2) contained
217 the true L_1 and L_2 values. For example, fish generated under regime 1 and occupying latitudes and
218 longitudes between 0° and 25° may have been re-aggregated via the GAM analysis into a *de facto*
219 ‘region’ ranging from 0° to 24° degrees for an “early” period of years 1 through 37; the parameters
220 of the VBGF were estimated on this per-strata basis, and the terminal lengths of the estimated
221 curve compared to those from which they were generated, in this case, regime 1. Fits from the
222 complementary *de facto* ‘region’ ranging from 24° to 50°, and/or a “late” period, would be
223 compared to whichever regime generated the majority of fish therein. An estimated endpoint from
224 a GAM-defined region was considered a match if the 95% confidence interval for it contained the
225 true value of L_1 or L_2 .

226 To facilitate comparison between the proposed GAM-based method and an extant approach,
227 we applied the sequential *t*-test analysis of regime shifts (STARS, Rodionov, 2004) using length-
228 at-age for age 6 to our simulated datasets for both spatial and temporal changes. The STARS
229 method was originally developed to detect climate regime shifts in time-series data, and was noted
230 for its sensitivity to changes towards the end of a series. The method examines the sequential
231 differences in the value of a *t*-distributed variable, and determines whether subsequent
measurements (at the next year or latitude, for example) exceed the expected range. We used a

minimum regime ‘length’ of five, meaning detected shifts between latitudes, longitudes or years must persist for at least five consecutive units, and the default p-value cutoff of 0.05. We believe this captures the timescale of regime shifts of interest to ecologists, and a significance cutoff frequently used in such analyses. From the STARS analysis of each dataset, we selected the breakpoint(s) with the largest positive “regime shift index”, which represents a cumulative sum of the normalized anomalies. This is qualitatively similar to the “largest first derivative” metric used in the proposed GAM-based method and, as in that case, was applied regardless of where the breakpoint was detected. We implemented the same steps, whereby the detected spatial and/or temporal breakpoint(s) were used to re-aggregate and estimate growth parameters, and the proportion of accuracy and coverage probabilities for L_1 , and L_2 tabulated.

2.4 Application to Northeast Pacific Sablefish

We obtained fishery-independent length and age data from the Bering Sea, Aleutian Islands, and Gulf of Alaska Sablefish Longline Survey (Rutecki et al., 2016) and the U.S. West Coast Groundfish Bottom Trawl Survey (Northwest Fisheries Science Center, 2019) conducted annually by the Alaska Fisheries Science Center and the Northwest Fisheries Science Center, respectively. We also obtained length and age records from the Canadian Department of Fisheries and Oceans (Wyeth et al., 2005); see

Table 1 for a summary of survey data used in the application. Data from each management area included measured length, sex, age, and the starting latitude and longitude, which determined the survey station. Due to computational constraints, and to avoid disproportionate influence of more heavily-sampled areas on breakpoint estimates, we randomly subsampled 15,000 total records from each of the three management areas. The subsampling was random with respect to latitude, longitude, age and sex, using the sample_n function from the package *dplyr* (Wickham et al., 2019).

We applied the method to identify spatial and temporal breakpoints for each sex separately at several key ages: age 4 (before length-at-50%-maturity for both males and females in all management areas), age 6 (after length-at-50%-maturity for both males and females in all management areas) and age 30, roughly the length at which sablefish are expected to obtain their maximum length (Johnson et al., 2015). Our sampling method produced a data set with an average of 1,315 age 4, 1,283 age 6, and 65 age 30 sablefish of each sex from each management area. Growth model fitting was performed using all available data from each of the three management areas (see Supplementary Table A3 for sample sizes). In constructing the GAM, we investigated the use of an AR1 temporal structure for the residual ϵ_t with lags of 1 to 3 years, but these models did not improve AICc over the initial model (without autoregressive structure).

We re-aggregated all data to match the breakpoints that appeared in the GAM analysis for key ages, as well as an ecosystem-based breakpoint at 145°W. We selected this breakpoint based on work by Waite and Mueter (2013) who used cluster analysis to delineate unique zones of chlorophyll-a variability, which has been shown to be influential in the sablefish recruitment process (Shotwell et al., 2014) but by definition such an effect is not detectable in our analysis that

271 only examines fish larger and/or older than recruits. The North Pacific Fishery Management
 272 Council uses 145°W, which includes a cluster of several seamounts in the Gulf of Alaska, to
 273 delineate a groundfish slope habitat conservation area (Siddon and Zador, 2018). We employed a
 274 stepwise exploration of whether estimates of L_∞ were significantly different between detected
 275 regions using the method and generated from this ecosystem break using the entire, non-sub-
 276 sampled dataset. [Asymptotic length was used to ease comparison between estimated values and
those used in the current assessments](#). This involved first aggregating and estimating the VBGF
 277 for ten unique spatiotemporal strata for each sex, defined by the one temporal and three spatial
 278 breakpoints found among the key ages selected for analysis using the GAM in addition to the break
 279 at the aforementioned ecosystem feature. To account for length-based selectivity, which is
 280 implemented only for the British Columbia data, we applied a penalty to the likelihood function
 281 as follows:

283 [Equation 6](#)
$$L(D|\theta) = \prod_i S_{L_i} \frac{1}{\sqrt{2\pi}\sigma a_i} e^{-(L_i - \hat{L}_i)/(2[\sigma a_i]^2)} / \int_{-\infty}^{\infty} S_l \frac{1}{\sqrt{2\pi}\sigma a_i} e^{-(\hat{L}_i - l)/(2[\sigma a_i]^2)} dl$$

284 where L_i is the observed length at a given age a_i , \hat{L}_i is the corresponding estimate based on VBGF
 285 parameters θ , S is a logistic selectivity function with parameter L_{50} , the length at which 50% of
 286 individuals (male or female) are fully selected, set to 52.976 cm (Samuel Johnson, SFU, pers.
 287 comm.)

288 [Equation 7](#)
$$S_L = \frac{1}{1 + \exp(L_{50} - L)}$$

289 As length-based selectivity is assumed constant in both the California Current and Alaskan
 290 assessments, S_L is set to 1.0 when fitting data points from those regions.

291 We then examined whether the 95% confidence intervals for L_∞ overlapped for any temporally-
 292 split datasets from the same region (e.g., region 1 female sablefish data before and during 2010
 293 and after 2010). If they did, we pooled the data for that region and sex for all years. In the second
 294 step, we examined if spatially-adjacent regions (from any time period) for the same sex had 95%
 295 confidence intervals for L_∞ that overlapped, and combined regions for which this was the case on
 296 a by-sex basis. This stepwise approach reduces unnecessary partitioning of the data into
 297 spatiotemporal strata that do not ultimately result in different estimates of L_∞ , and allowed us to
 298 examine whether any of our detected breakpoints or the *post hoc* ecosystem split was informative
 299 regarding growth estimates. Once the most parsimonious structure was identified through this
 300 method, we generated predicted lengths-at-age for the entire dataset.

301

302 **3 Results**

303 *3.1 Simulation Study*

304 The simulation study demonstrated that the first-derivative GAM-based method is able to
 305 detect both spatial and temporal breakpoints correctly in the majority of scenarios, with the
 306 exception a scenario where the spatial break occurred near the edge of the simulated spatial extent
 307 at 48° longitude, where it only detected the break location correctly in 15% of simulations. [Figure
4 displays the coverage probabilities for the 95% confidence intervals and proportion of](#)

309 simulations wherein the correct breakpoint was detected perfectly or with a “relaxed” criteria
310 (within 2 degrees, roughly 220 km, or 2 years), demonstrating the success rate of the method across
311 a variety of simulations. Supplementary Figure A3 and A4 presents a histogram of detected breaks
312 for each scenario.

313 For all scenarios, the method achieved the highest coverage probabilities for the length-at-age
314 0 (L_1) [48%-97% coverage for three scenarios and 27% in the scenario with overlap]. Coverage
315 probabilities for length-at-age 15 (L_2) were slightly lower [43% - 74% for three scenarios and 16%
316 in the scenario with overlap]. In terms of spatial breakpoint detection, there was not a qualitatively
317 strong difference in the method’s ability to correctly detect latitudinal vs. longitudinal breakpoints
318 across scenarios. Our GAM-based method correctly detected the lack of a breakpoint in 86% of
319 simulations without breaks; there was no discernable pattern to the spurious spatial breakpoints
320 identified in the remaining simulations. The method did less well at detecting the accurate
321 breakpoints for scenario 4 (a “true” spatial break at 48°), assigning the break between 45° and 50°
322 longitude in 100% of simulations; similarly, for the scenario with a single breakpoint at 25°, the
323 GAM-based method was 100% accurate when the criteria were relaxed to include breaks from 24°
324 to 26°. Relaxing the criteria in this manner increased the method’s accuracy to over 90% for all
325 scenarios except one (Figure 4c). We computed the mean absolute error in both L_1 and L_2 estimates
326 across scenarios and found the maximum error to be 1.84 cm for L_1 and 6.98 cm L_2 , both obtained
327 in scenario 1. Finally, we did not find the method’s accuracy sensitive to either halving or reducing
328 the sample size by 25%; see Supplementary Table A2.

329 3.2 Comparison to STARS Method

330 The STARS method (Supplementary Figure A1) was inferior to the proposed GAM-based method
331 at detecting spatial or temporal break points for all simulated scenarios, with a slight exception for
332 the break at edge case (scenario 4). For all other scenarios, the STARS method performed up to
333 90% worse than the proposed GAM-based method at detecting latitude and longitude breaks, and
334 20% worse at detecting year breaks. It also performed worse in terms of the coverage probability
335 of L_1 (63% vs 67% for the GAM-based method) and L_2 (18% vs 52%), and did slightly better than
336 the proposed method in detecting the break-at-edge, though only at 31% (vs 11%).

337 3.3 Application to NE Pacific Sablefish

338 The latitude smoother suggested a generally increasing cline in length-at-age with latitude,
339 with a significant breakpoint around 50°N (approximately the northern end of Vancouver Island,
340 Canada) detected when the GAM was fit for age four and six sablefish (Figure 5c, 6c;
341 Supplementary Figures A4, A7, A9). North of this breakpoint, female L_2 estimates were
342 consistently larger than 70 cm, where they averaged 65 cm south of it. Both age six and age 30
343 female sablefish identified a breakpoint at 36°N (approximately Monterey, CA, USA). Both males
344 and females obtained the lowest estimated L_2 south of this breakpoint, at 55 cm for males and 60
345 cm for females. In all GAM-detected regions, L_∞ was higher for female sablefish than males, and
346 the resultant L_2 differed between regions within sexes by up to 26%. The temporal smoother did
347 not exhibit a strong one-way trend, and was flat for age-30 fish of both sexes, though it did detect

348 a break in 2009-2010 for both sexes of age 4 and 6 sablefish. Parameter estimation at this temporal
349 stratification generated 95% confidence intervals for L_∞ which overlapped for males within all
350 regions and for females in region 5 (Supplementary Figure A14). The number of spatiotemporal
351 strata was reduced to 14 after combining years of data for region-sex combinations where overlap
352 was found in the second phase. Once re-aggregated and re-estimated, we did not find overlapping
353 confidence intervals for L_∞ for any adjacent regions, so this set of specifications (five spatial
354 regions for both sexes, and a temporal break for females in regions 1 through 4) was retained as
355 our final spatiotemporal stratification. The stratification consists of three regions bounded on their
356 western border by a break at 130°W; from south to north, these regions (labeled 1, 2 and 3 on
357 Figure 7) are defined by latitudes 36°N and 50°N. They correspond generally to Monterey, CA and
358 the northern tip of Vancouver Island, BC. Region 4 is the area between 130°W and the ecosystem
359 break at 145°W (roughly Cordova, AK). Datapoints collected to the west of the ecosystem break
360 are assigned to region 5.

361

362 4 Discussion

363 Empirical work has suggested that somatic growth in fishes follows ecosystem gradients rather
364 than management boundaries (Pörtner and Knust, 2007; Taylor et al., 2018). The ongoing
365 emphasis on ecosystem-based fisheries management calls for the analysis of fish stocks (ideally in
366 a multi-species context, but also as single species) at meaningful spatial scales, across which
367 changes can be detected. Our goal was to investigate the performance a method to improve
368 detection of large-scale patterns in fish growth and apply it to length-at-age data from the Northeast
369 Pacific sablefish. Our method determined that the current management scale (three political breaks
370 at national boundaries) is incongruent with the underlying pattern of variation in sablefish growth.
371 We discerned that the spatial variation in sablefish growth corresponds well with major
372 oceanographic features, principally the splitting of two major ocean features and the edge of a
373 highly productive zone. Below, we discuss the results of the simulation study and provide further
374 guidance on how researchers could apply our proposed method to new datasets. We then discuss
375 the results found during the application to northeast Pacific sablefish, with respect to ecosystem
376 concerns.

377 4.1 Implications of Simulation Results

378 Our GAM-based method indicated tradeoffs between the accuracy of breakpoint detection and
379 resultant coverage probabilities in the estimated growth curve, as well as large differences in the
380 coverage probabilities of fish length at younger versus older ages. We find it encouraging that the
381 approach could correctly detect breakpoints for the scenario with overlapping ranges, which is
382 likely more like real-world fish populations than the singular, immediate breakpoints simulated in
383 other scenarios. However, the assigned ‘zonation’ of these populations necessarily combined fish
384 with contrasting growth curves into a single dataset for estimation and resulted in a loss in accuracy
385 (coverage probability) for the endpoints of the growth curve. Alternate GAM-based methods, such
386 as the clustering approach applied in Winton et al. (2014), have also demonstrated that detecting
387 spatial structure through a spatially explicit process can reveal distinct sub-areas in fish traits (e.g.

388 mortality). That study also found that models did not necessarily require explicit ecosystem data
389 (like temperature) to perform as well as models with only spatial information.

390 We suggest that our method be used as a tool to guide the identification of general zones
391 between which growth could vary, and not take detected breakpoints as the absolute truth.
392 Importantly, suggestions of spatial breakpoints produced by the method should necessarily be
393 considered in the context of the ecosystem, and prior knowledge of how the fishery at hand
394 responds to features (e.g., temperature, depth) which vary with latitude and/or longitude. Absent
395 an ecosystem-wide analysis, strong directional trends in any generalized additive term (such as the
396 positive trend with latitude observed here) or a breakpoint at the edge of the study area can be
397 indicative of a change somewhere in the margins and extend the reach of future survey designs.

398 The method performed best for both performance metrics for the scenario in which growth
399 regimes 1 and 2 overlapped in space (which had the advantage of being ‘matched’ whenever the
400 detected breakpoint fell within the range of overlap, 20° to 25°). The most commonly detected
401 breakpoint in latitude and longitude for that scenario, before rounding, was the midpoint of this
402 range (22.5°), likely an artifact of the penalization function within the GAM, which seeks to
403 minimize curvature on either side of a given knot (i.e., the breakpoint). This penalization function
404 controls the degree of smoothness on the spline and can lead to fitting overly-complex models
405 when unchecked (Wood, 2003). Since the purpose of this analysis was diagnostic (the detection of
406 where the spline is changing the most), we were able to avoid undue influence from this parameter
407 by a) selecting only the value corresponding to the maximum first derivative and b) that had
408 confidence intervals not containing zero, which are common in highly curved splines. **We also**
409 **chose to use only the maximum absolute value of the derivative to avoid splitting the spatio-**
410 **temporal surface into many small zones, which may have led to problems of small sample size, or**
411 **ultimately be unrealistic to implement in a population dynamics model of the fishery and stock.**

412 We detected spurious spatial or temporal breaks in ~10% of simulations for which no
413 breakpoints were present. However, some erroneous detection can be expected considering the
414 inherent noise in our datasets, and that there is no minimum threshold for breakpoint detection; a
415 single, small derivative among many zeros that did not have a confidence interval containing zero
416 could be ‘picked’. This observation partially motivated the two-phase procedure employed for the
417 sablefish application, so it is likely that such erroneous detection would be reduced if overlapping
418 growth estimates were disregarded (our simulation analysis investigated the accuracy of the first
419 stage). We evaluated if an autoregressive structure improved our simulation models as length-at-
420 age can be time-dependent, but it did not; this may not be the case for other fisheries.

421 In addition, we did not simulate nor consider error or bias in the aging (i.e., otolith reading)
422 process (Cope and Punt, 2007), which would potentially introduce uncertainty in breakpoint
423 detection. **Based on aging workshops conducted for sablefish, we consider aging results used in**
424 **the case study to be roughly comparable between regions (Fenske et al., 2019).** With these caveats
425 in mind, we envision (and demonstrate) using the method as a tool to identify general regions and
426 periods of change in fish length-at-age, which will necessarily be evaluated against pre-existing
427 knowledge of the fish population and its ecosystem.

Neither the GAM-based nor the STARS approach is appropriate for extrapolation (prediction beyond the range of covariates, or outside of the ecosystem, used in model fitting), particularly because they use indirect variables such as latitude which may have nonlinear or inverted relationships with fish physiology in other ecosystems (Austin, 2002). It is likely there are thresholds in, or types of, spatiotemporal growth variation that will be poorly detected by most methods, which we see as a promising area for future research.

4.2 Implications of detected breakpoints for Northeast Pacific Sablefish

Our evaluation of size-at-age for NE Pacific sablefish was directly motivated by the notion that sablefish growth may vary at a scale that differs from present management boundaries. For NE Pacific sablefish, we applied the method to each sex separately at a set of key biological ages and determined that sablefish length-at-age differs most significantly across five regions, whose boundaries can be defined by major oceanographic features (the Southern California Bight, and the bifurcation of the North Pacific Current) as well as a known ecosystem boundary in the Gulf of Alaska. It is evident from this and previous work (Echave et al., 2012; Gertseva et al., 2017; McDevitt, 1990) that there is some level of variation in sablefish growth, whether in the growth rates themselves or the spatiotemporal scale at which variation in growth occurs. Previous work with sablefish data has utilized an *a priori* method, wherein length and age data were aggregated into pre-hypothesized spatial zones and fitted VBGF curves were compared using Akaike's Information Criterion. This 'information-theoretic' (Guthery et al., 2003) method is fairly straightforward computationally, and has been implemented separately for the California Current (Gertseva et al., 2017) and Alaska federal sablefish fisheries (Echave et al., 2012; McDevitt, 1990). The California Current analysis identified a statistically significant break in VBGF parameters for sablefish at approximately 36° N, between Point Conception and Monterey, CA, with additional evidence for an increasing cline in L_∞ with increasing latitude and a general increase in estimated L_∞ and L_2 for more northerly regions. These results mirror the trend in our latitudinal smoother (Figure 5 and 6) and our detected breakpoint at 36°N (Figure 7), which is incidentally a management sub-boundary used by the US Pacific Fishery Management Council. That work also found an increase in k estimates for areas sampled south of the Vancouver area (ca. 49°N), which was posited to be the result of samples coming from the "southern end of a faster-growing northern stock", a suggestion supported by our findings of another breakpoint at 50°N. Preliminary analyses of sablefish tagged in Alaska suggest that the British Columbia management area exports fish into the California Current and Gulf of Alaska, a diffusion pattern that could potentially taper off with decreasing latitude; the distance between Vancouver, B.C. and Monterey, C.A. is approximately three times the mean great-circle movement distance for sablefish determined by Hanselman et al. (2015), which is a measure of the shortest possible distance traveled between tagged and recovered animals. Gertseva et al. (2017) described how sablefish have been shown to be highly mobile, with ontogenetic movements off the coastal shelf; such combined, complex life patterns could yield higher growth rates in northern latitudes that interact with a more generalized shelf-slope pattern of ontogenetic movement observed in groundfish overall.

468 There are several noteworthy trends in the stratified growth estimates (

469 Figure 8) that warrant future research. Firstly, the *post hoc* incorporation of a spatial break at

470 145°W based on ecosystem data was not ruled out during the significance testing of L_∞ . This

471 supports the notion that environmental features may result in variations in growth, and that the

472 proposed GAM-based method is amenable to improvements based on the incorporation of climate

473 or ecosystem knowledge. Additionally, both latitudinal breakpoints are loosely associated with

474 significant oceanographic features, namely start of the southern California Bight at Point

475 Conception (~34°N) and the bifurcation of the North Pacific Current, which splits into the Alaska

476 and California currents as it approaches the west coast of North America. **The breakpoint at 36°N**

477 **is slightly north of the beginning of the bight, but also characterized by dynamic, mostly southward**

478 **floor in the nearshore environment.** The formal location of the North Pacific bifurcation varies,

479 but is generally centered off the coast of British Columbia (Cummins and Freeland, 2007; Figure

480 7). In common with the ecosystem split identified in the Gulf of Alaska, these oceanographic

481 features lead to distinct zones of productivity (Kim et al., 2009; Mackas et al., 2011) that could

482 influence resource availability and subsequent growth.

483 The temporal break in year 2010 was conserved (supported by significantly different L_∞

484 estimates) only for female fish, and more so in the southerly latitudes (such as regions 1 through

485 4, which are mostly comprised of California Current data), and exist along a steeper north-south

486 cline. We note, however, that the procedure used to eliminate ‘overlapping’ L_∞ estimates

487 concerned only statistical differences in values (and are therefore sensitive to sample sizes). The

488 biological significance of these values should need to be investigated in the context of fecundity

489 and length-weight differences between regions.

490 Preliminary analyses of sablefish movement rates from tagging data from Alaska (as analyzed

491 in Hanselman et al., 2015) indicate that male sablefish seem to move more frequently to and from

492 sea mounts, which are situated within the GAM-defined regions identified here. There are several

493 possibilities for why female sablefish seem to exhibit finer spatiotemporal structure in growth.

494 Empirical work in Canada (Mason et al., 1983) that examined early life history of fishery-caught

495 coastal sablefish observed a slight cline in mean fork length with increasing latitude, although the

496 sex ratio within the study was biased towards females. That study suggested that selectivity for

497 female sablefish may be higher due to higher congregating or feeding activity, in addition to the

498 fact that females grow larger and are likely preferentially targeted in the commercial fishery in

499 BC, which is also true for the fixed-gear fisheries in the California Current (Johnson et al., 2015).

500 This could render females more sensitive to changes in fisher behavior, such as the implementation

501 of catch shares off the US west coast in 2011. Expanding the method to allow for detection of

502 multiple spatial and/or temporal breaks at once may enable further investigation of this

503 phenomenon, although it may lead to the creation of spurious regions with insignificant difference

504 in growth parameters, as observed in the first phase of the case study.

505 A plausible scenario that would generate our observed results could be that changes in fisher

506 behavior or climate in the last ~10 years caused female sablefish to move northward in greater

507 numbers, or simply experience size-based truncations in regions to the east of 145 due to fishing

508 pressure. Each of these phenomena would have an inverse effect on resultant size-at-age, with fish
509 entering the northern ecosystem tending to grow larger and high, persistent fishing pressure in any
510 region leading to truncations in terminal size. Because we only detected slight declines size-at-age
511 between time periods for female sablefish, it is possible that either fishery-related effects simply
512 have not lasted long enough to be strongly evident, or such effects are being counteracted by more
513 fish entering ecosystems favorable to higher terminal sizes. A closer examination of sex-related
514 movement would be useful towards this understanding.

515 Consideration of temporal variation in sablefish growth is further complicated by the
516 exploitation history of the fishery, which has steadily moved north- and west-ward in the California
517 Current and Alaska over the last several decades, encountering ‘larger’ fish with subsequent
518 expansion (Pacific Fisheries Management Council (PFMC), 2013) This suggests that differences
519 in mean length across the region could be attributable to different degrees, durations, or patterns
520 of fishing pressure (Hilborn and Minte-Vera, 2008), interacting with inherent growth variation to
521 produce such spatiotemporal patterns. A principal conclusion of Stawitz et al. (2015) was that the
522 form of sablefish growth variation differed among ecosystems, wherein the California Current is
523 a more climactically variable ecosystem. Such ecosystem-driven trends may be diluted when
524 analyzing the data as a composite, as in our study. Notably, our temporal smoother did not produce
525 a distinct annual or cyclic trend. Methods that consider the space and time components co-
526 dependently (as in vectorized auto-regressive spatiotemporal models, Thorson, 2019a) may
527 strengthen the ability to disentangle such trends, and also to consider covarying spatial effects (e.g.
528 near- and offshore).

529

530 **Acknowledgments**

531 The authors would like to thank Owen Hamel and Christine Stawitz of the Northwest Fisheries
532 Science Center and two anonymous reviewers for their thoughtful comments that greatly improved
533 this manuscript. We’d like to thank John Best (SAFS) for suggesting the GAM derivative method
534 as a possible technique, and for the entire Pacific Sablefish Transboundary Assessment Team for
535 their support and feedback on this work. This publication was [partially] funded by the Joint
536 Institute for the Study of the Atmosphere and Ocean (JISAO) under NOAA Cooperative agreement
537 No. NA15OAR4320063, Contribution No. 2019-1030.

Figures

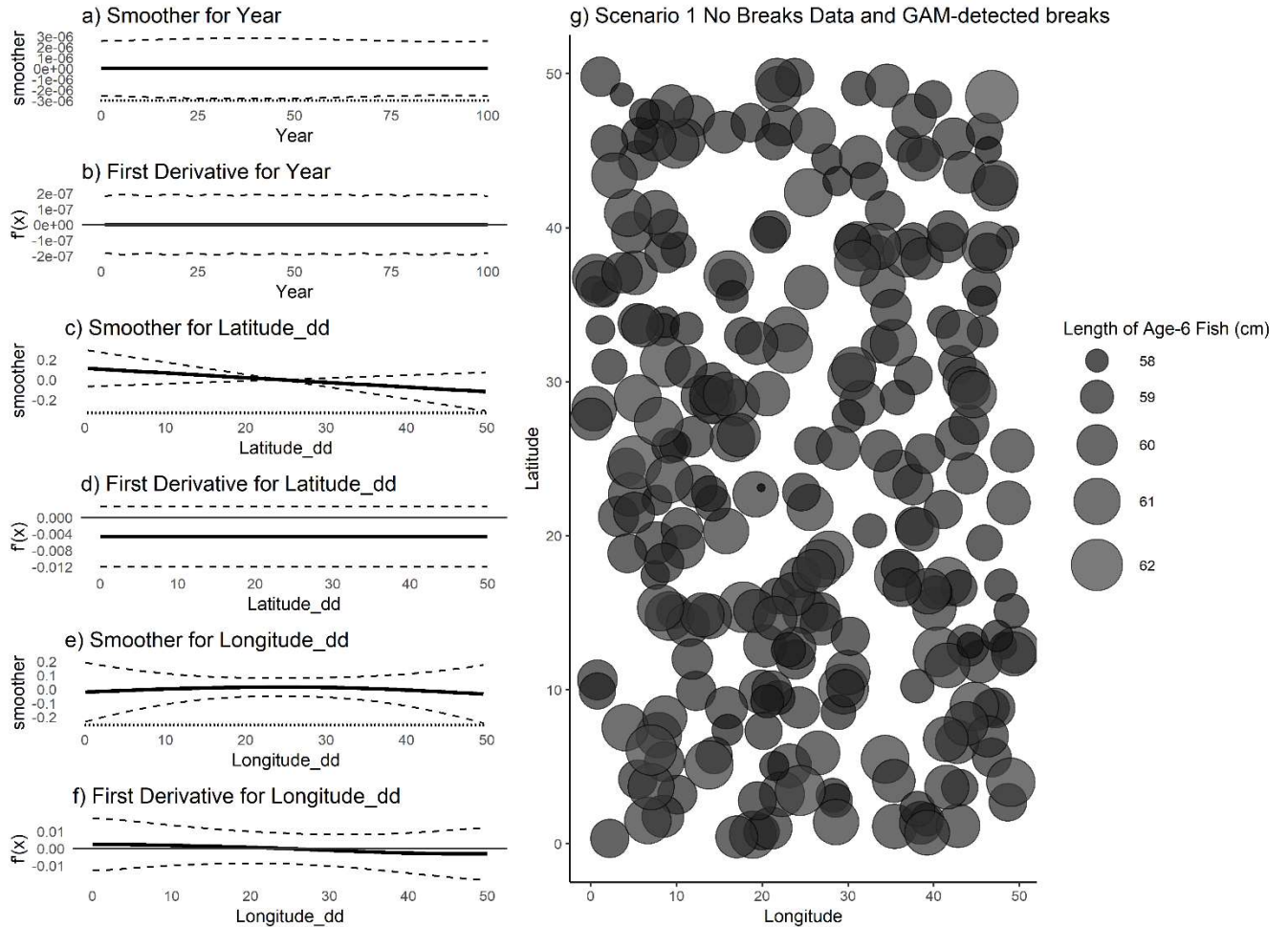


Figure 1. (a,c,e) raw value of GAM smoothers for Year, Latitude and Longitude; (b,d,f) mean (black line) and 95% CI (black dashed lines) of first derivative of the smoothers; (g) map of age-6 fish for a single simulated dataset with no designated spatial or temporal breaks. No break points were detected by the GAM.

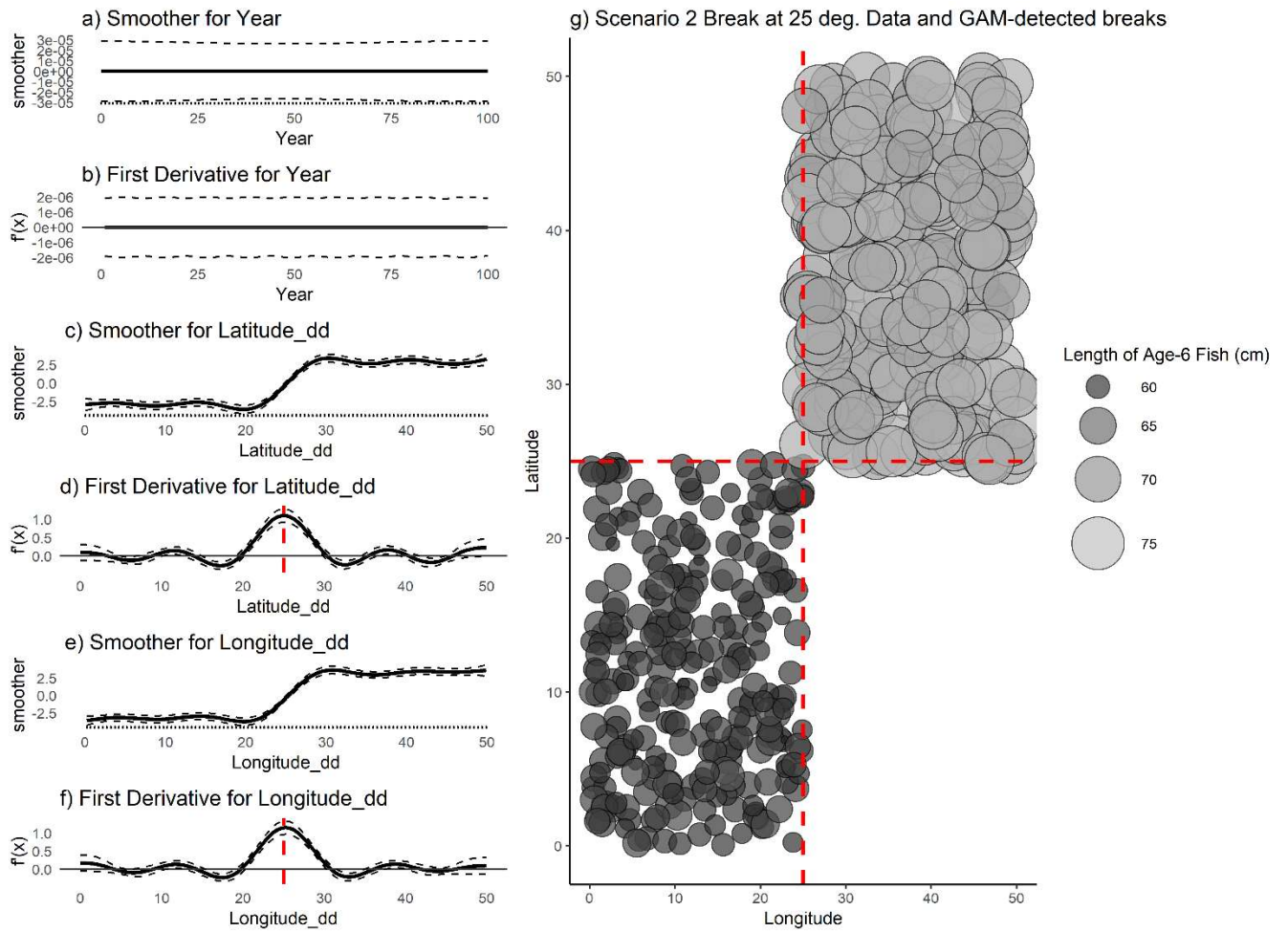


Figure 2. (a,c,e) raw value of smoothers (fitted regression splines) for year, latitude, and longitude; (b,d,f) mean (black line) and 95% CI (black dashed lines) of the first derivatives of the smoothers; (g) map of age-6 fish for a single simulated dataset with a single, symmetrical break at 25° latitude and longitude. Dashed red lines indicate detected break points, which are the maximum value obtained for this data set and do not have a confidence interval that contains zero.

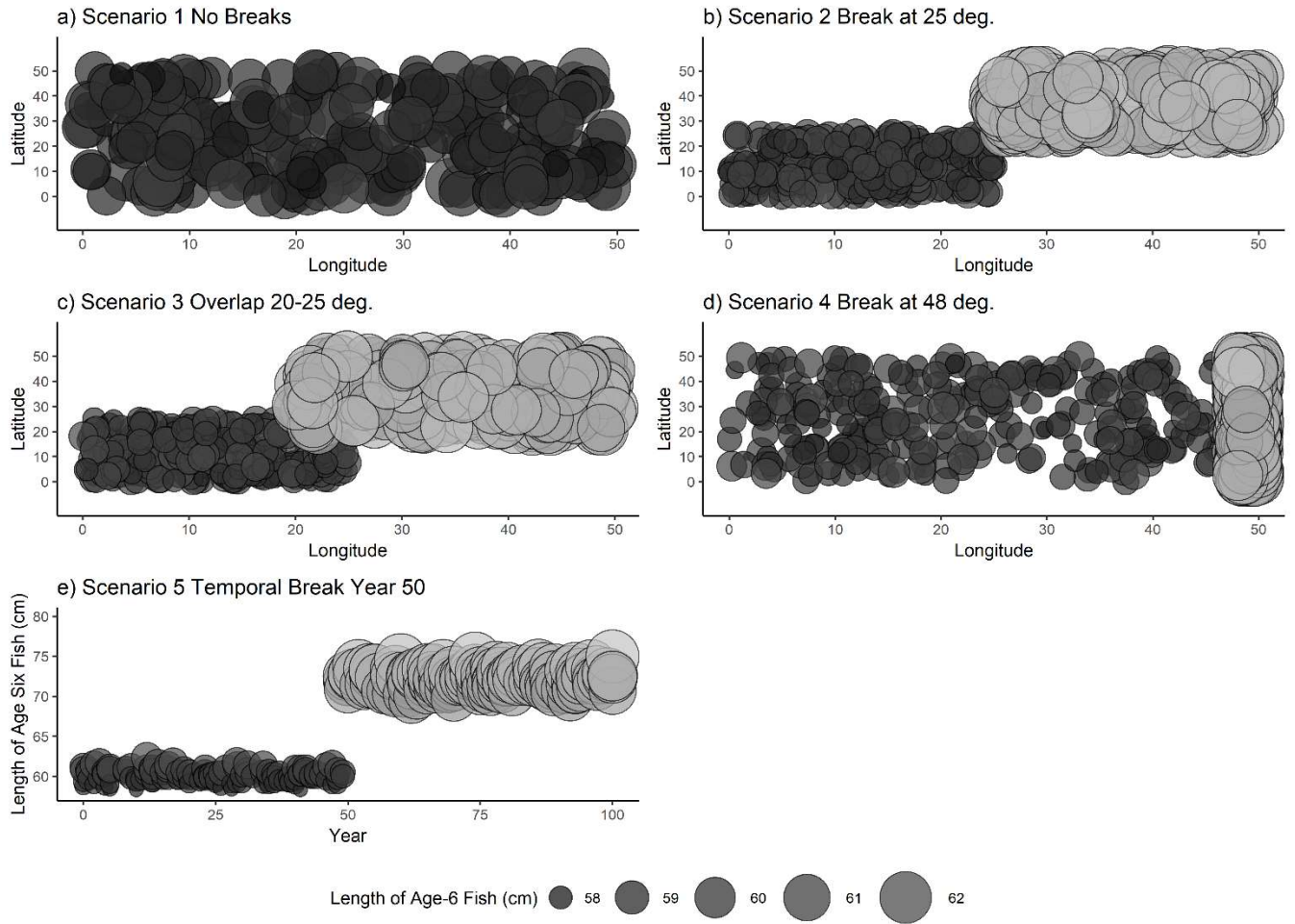


Figure 3. Example dataset for each of the scenarios in Table 2. For each of the five scenarios, points represent the length and location of a single simulated fish at age six. Fish locations (latitudes and longitudes) were sampled from a uniform distribution of the boundaries indicated in Table 2.

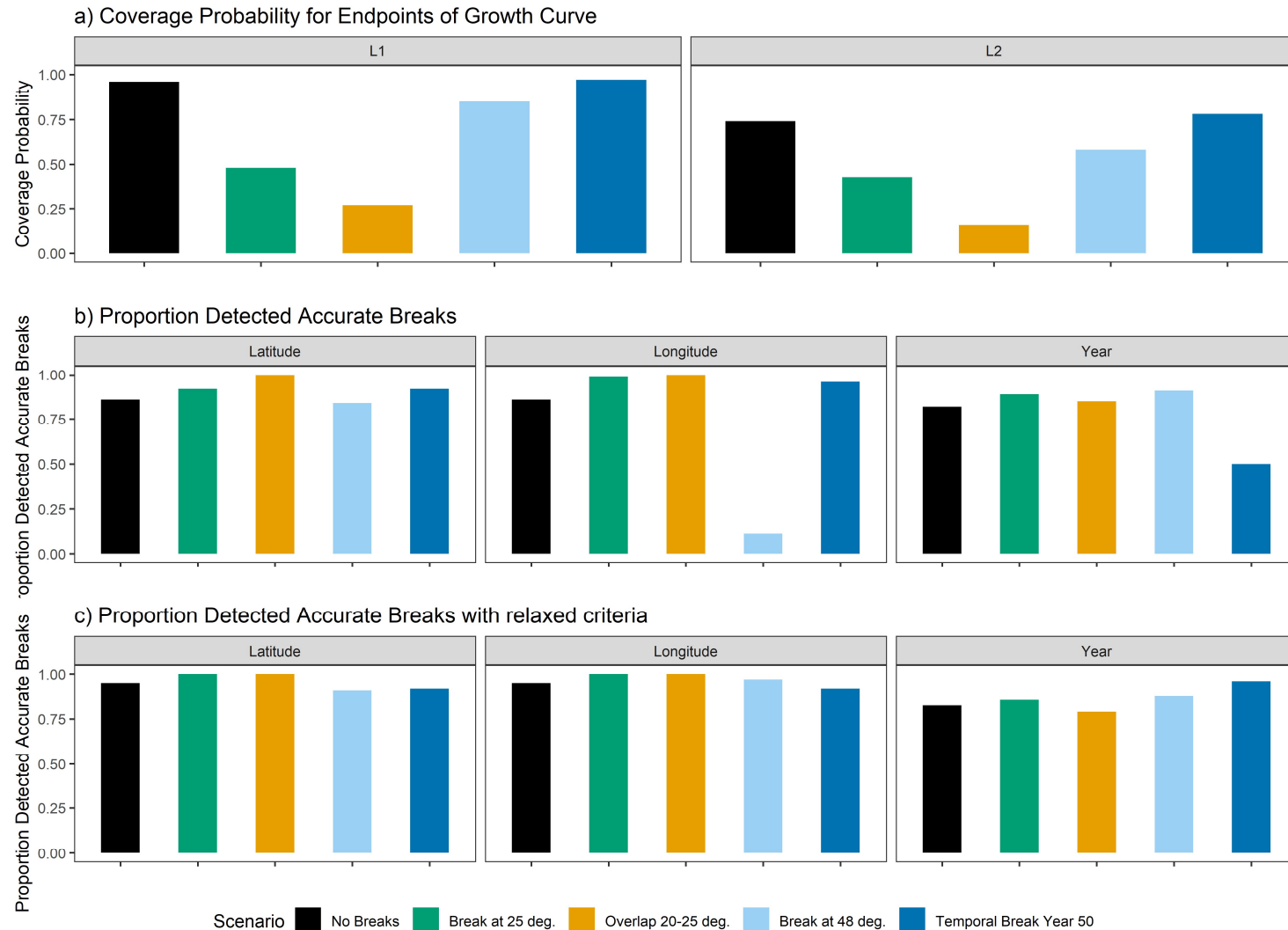


Figure 4. a) coverage probabilities for the endpoints of the growth curve, L_1 (left) and L_2 (right); b) proportion of 100 simulations for each spatial scenario wherein the correct latitudinal breaks (left), or longitudinal breaks (center) or temporal break (right) were detected. c) the same as b) but with the criteria for a ‘match’ relaxed to include breakpoints within two degrees or years of the truth.

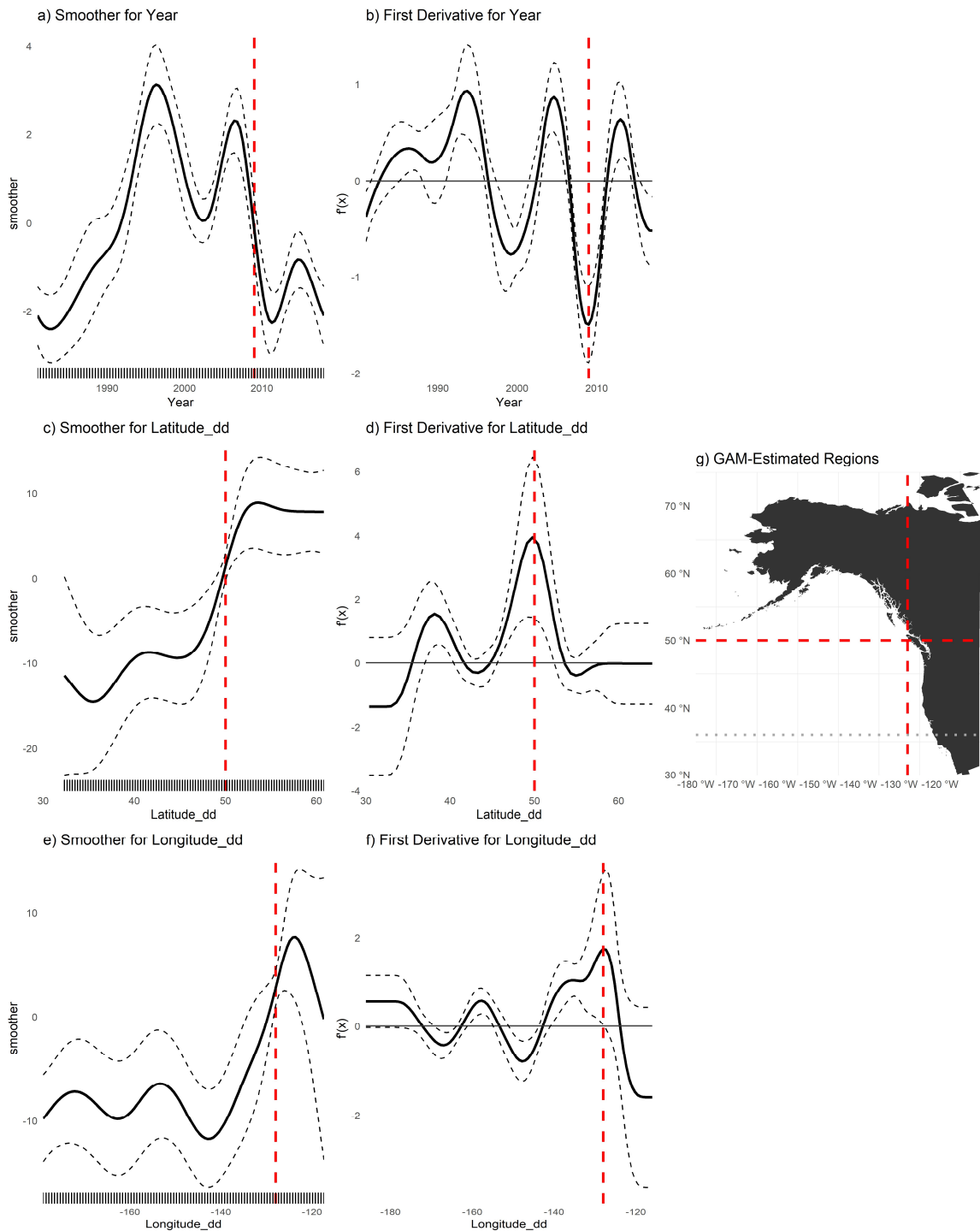


Figure 5. (a,c,e) Plots of smoothers (fitted regression splines) for year, latitude, and longitude, and first derivatives thereof for female age four sablefish (b,d,f). On a-f, vertical dashed lines indicate latitudes, longitudes or years that correspond to the highest first derivative and had a confidence interval that did not include zero. g) map with model-detected breakpoints (red dashed lines) and breakpoints detected for other ages (grey dotted line).

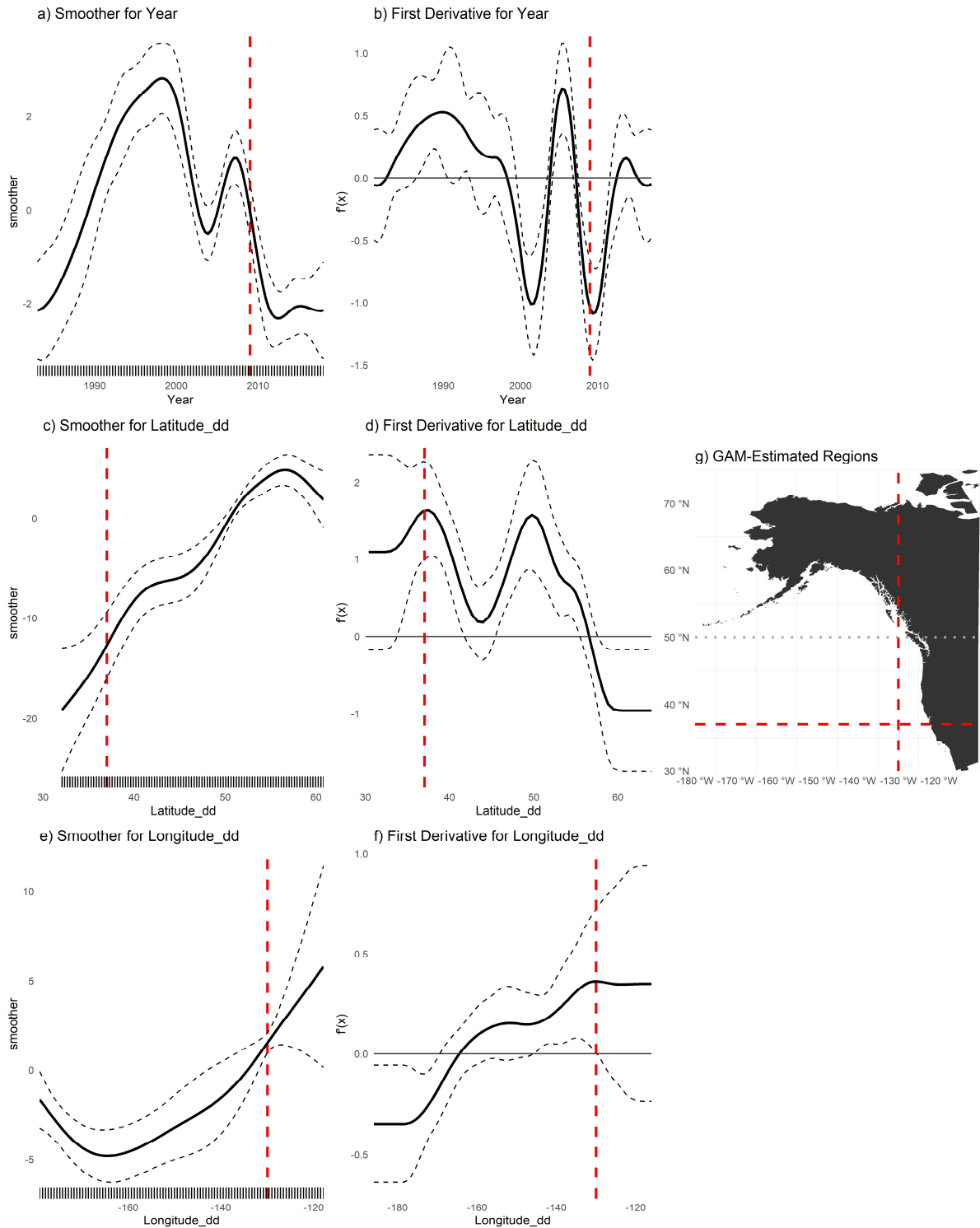


Figure 6. (a,c,e) Plots of smoothers (fitted regression splines) for Year, Latitude, and Longitude, and first derivatives thereof for female age six sablefish (b,d,f). On a-f, vertical dashed lines indicate latitudes, longitudes or years that corresponded to the highest first derivative and had a confidence interval that did not include zero. g) map with model-detected breakpoints (red dashed lines) and breakpoints detected for other ages (grey dotted line).

Northeast Pacific

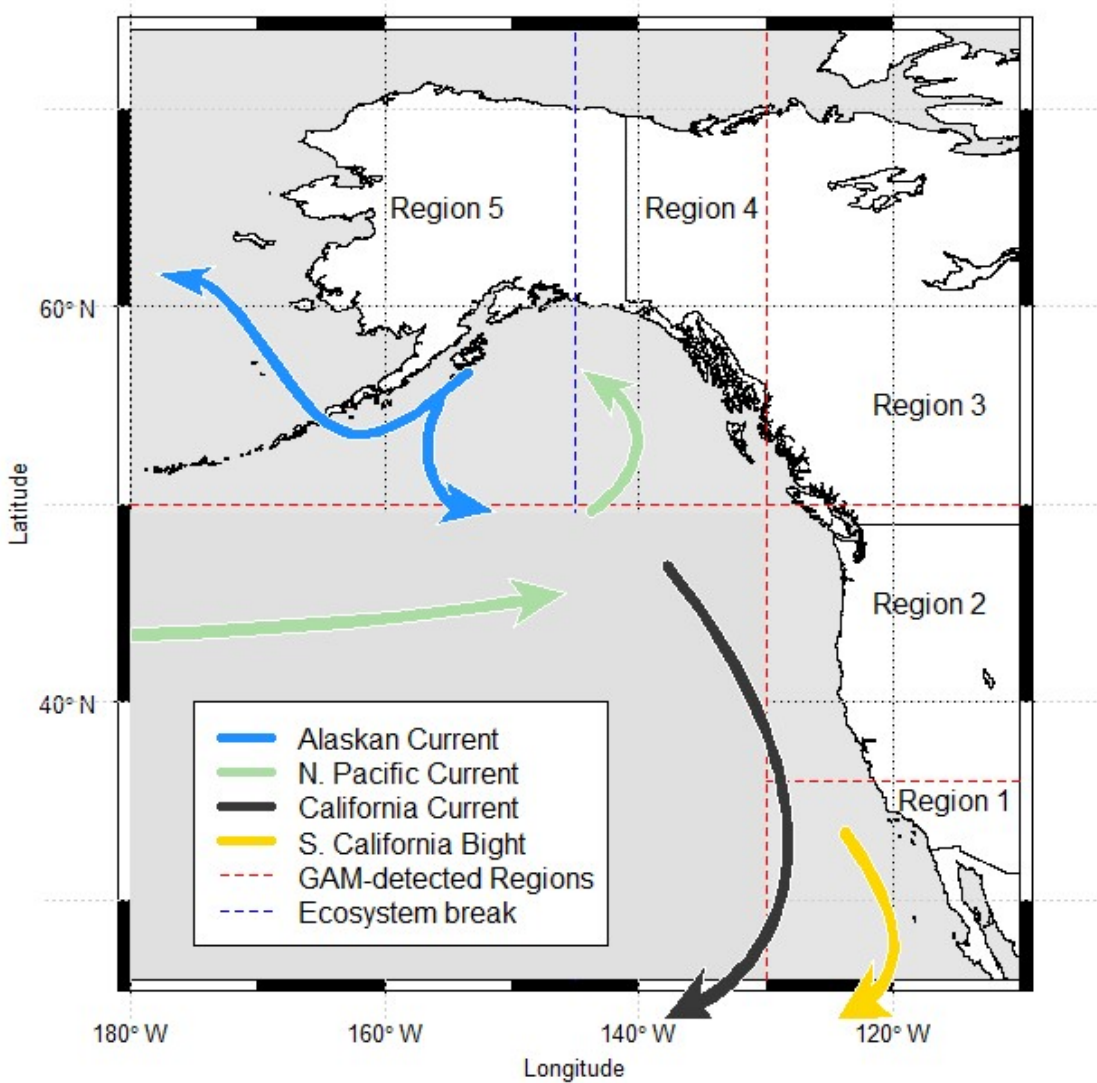


Figure 7. Method-detected breakpoints (red dashed lines) and ecosystem-based break (blue dashed lines) used to delineate growth regions for sablefish. Map made in R using current data from: https://data.amerigeoss.org/en_AU/dataset/major-ocean-currents-arrowpolys-30m-85

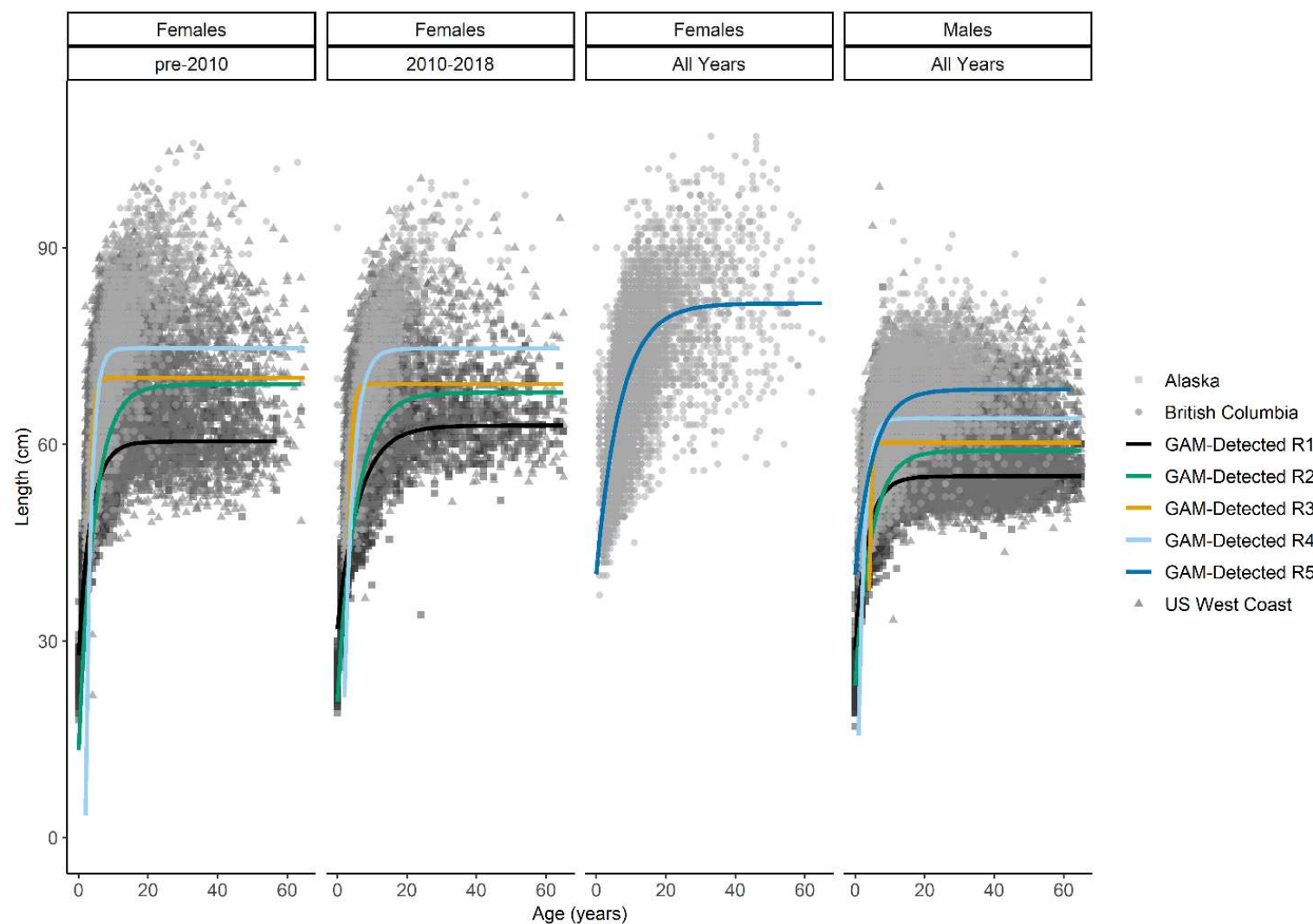


Figure 8. Fits of von Bertalanffy growth function (colored lines) to data at the final spatiotemporal aggregation (panels). Points are raw survey data with color and shape corresponding to their source.

Tables

Region	Survey Method	Sample size used in this analysis to fit GAM		VBGF parameters from recent stock assessments							
		M	F	L_∞ (cm)		k (years ⁻¹)		t_0 (years)			
				M	F	M	F	M	F		
West Coast of US (Johnson et al., 2015)	Trawl on chartered commercial fishing vessels	7,778	7,222	57	64	0.41	0.32	0 (fixed)	0 (fixed)		
British Columbia	Stratified trap survey	6,912	8,088	68.99	72.00	0.29	0.25	^	^		
Alaska Federal (Hanselman et al., 2017)	Longline on chartered commercial fishing vessels	6,818	8,182	*67.8 *65.3	*80.2 *75.6	*0.29 *0.28	*0.22 *0.21	**2.27	**1.95		

Table 1. Overview of survey methods, data available and most recent VBGF parameters used for sablefish in stock assessments.

*Time-blocked VBGF parameters for Alaska Federal assessment 1996-2018

†Time-blocked VBGF parameters for Alaska Federal assessment from 1960-1995 (Hanselman et al., 2017)

^The BC assessment fixes length at age-1 to 32.5cm.

Scenario Number	Scenario Description	Stratification
1	No spatial breaks	Latitude and Longitude $\sim U[0,50]$, all fish under regime 1
2	Single, spatial break in middle of range, with no overlap	Latitude and Longitude $\sim U[0,25]$ under regime 1; Latitude and Longitude $\sim U[25,50]$ under regime 2
3	Some overlap between regions	Latitude and Longitude $\sim U[0,25]$ under regime 1; Latitude and Longitude $\sim U[20,50]$ under regime 2
4	Single spatial break at edge of range with no overlap	Latitude $\sim U[0,50]$ for regimes 1 and 2; Longitude $\sim U[0,48]$ for regime 1 Longitude $\sim U[48,50]$ for regime 2
5	Single temporal break at year 50 (of 100); no spatial variability	Latitude and Longitude $\sim U[0,50]$, all fish under regime 1 from years 0 to 49 and regime 2 thereafter

Table 2. Summary of simulation scenarios used to test the proposed GAM-based method given various extents of spatial growth variation, and a single temporal scenario.

Region	Sex	Period	Sample size used to fit GAM	Estimated VGBF Parameters			Corresponding estimated endpoints of growth curve	
				L_∞ (cm)	k (years ⁻¹)	t_0 (years)	L_1 (cm)	L_2 (cm)
R1	Female	Early	985	60.44	0.29	-2.15	32.21	60.43
R1	Female	Late	1,101	62.86	0.16	-4.31	34.22	62.63
R1	Male	All Years	2,048	55.11	0.28	-2.59	32.08	55.11
R2	Female	Early	8,412	69.14	0.22	-0.96	19.22	69.08
R2	Female	Late	5,557	67.91	0.19	-1.96	24.84	67.73
R2	Male	All Years	14,990	59.04	0.21	-2.34	26.83	58.98
R3	Female	Early	2,517	70.15	1.29	2.41	61.09*	70.15
R3	Female	Late	852	69.21	1.18	2.32	59.72*	69.21
R3	Male	All Years	2,698	60.26	2.12	3.54	37.56*	60.26
R4	Female	Early	9,411	74.66	0.66	1.93	55.49*	74.66
R4	Female	Late	4,155	74.62	0.39	1.14	50.37*	74.62
R4	Male	All Years	11,640	63.94	0.58	0.52	55.4*	63.94
R5	Female	All Years	13,212	81.5	0.14	-4.74	43.03	80.94
R5	Male	All Years	10,411	68.36	0.2	-4.51	42.82	68.28

Table 3. Description of final spatiotemporal regions, and the sex-specific growth parameters estimated in the analysis. The Region column corresponds to regions depicted in Figure 7, with “early” period being observations before or during 2010, where applicable. Parameter estimates are those used to plot fitted curves in

Figure 8. *Age 0.5 yrs was used to report L_1 estimates, except for values from Regions 3 and 4 for which L_1 corresponds to lengths at age 4.

References

- Adams, G.D. Leaf, R.T., Ballenger, J.C., Arnott, S.A., McDonough, C.J., 2018. Spatial variability in the growth of Sheepshead (*Archosargus probatocephalus*) in the Southeast US: Implications for assessment and management. *Fish. Res.* 206, 35–43.
<https://doi.org/10.1016/j.fishres.2018.04.023>
- Austin, M.P., 2002. Spatial prediction of species distribution: An interface between ecological theory and statistical modelling. *Ecol. Modell.* [https://doi.org/10.1016/S0304-3800\(02\)00205-3](https://doi.org/10.1016/S0304-3800(02)00205-3)
- Beck, K.K., Fletcher, M.S., Gadd, P.S., Heijnis, H., Saunders, K.M., Simpson, G.L., Zawadzki, A., 2018. Variance and rate-of-change as early warning signals for a critical transition in an aquatic ecosystem state: a test case from Tasmania, Australia. *J. Geophys. Res. Biogeosciences.* <https://doi.org/10.1002/2017JG004135>
- Cope, J.M., Punt, A.E., 2007. Erratum: Admitting ageing error when fitting growth curves: an example using the von Bertalanffy growth function with random effects. *Can. J. Fish. Aquat. Sci.* <https://doi.org/10.1139/f07-095>
- Cummins, P.F., Freeland, H.J., 2007. Variability of the North Pacific Current and its bifurcation. *Prog. Oceanogr.* 75, 253–265. <https://doi.org/10.1016/j.pocean.2007.08.006>
- Echave, K.B., Hanselman, D.H., Adkison, M.D., Sigler, M.F., 2012. Interdecadal change in growth of sablefish (*Anoplopoma fimbria*) in the Northeast Pacific ocean. *Fish. Bull.* 110, 361–374.
- Fenske, K.H., Berger, A.M., Connors, B., Cope, J., Cox, S.P., Haltuch, M., Hanselman, D.H., Kapur, M., Lacko, L., Lunsford, C., Rodgveller, C., Williams, B., 2019. Report on the 2018 International Sablefish Workshop. U.S. Dep. Commer., NOAA Tech. Memo. (No. NMFS-AFSC-387). Juneau, AK. <https://www.afsc.noaa.gov/Publications/AFSC-TM/NOAA-TM-AFSC-387.pdf>
- Gertseva, V., Matson, S.E., Cope, J., 2017. Spatial growth variability in marine fish: Example from Northeast Pacific groundfish. *ICES J. Mar. Sci.* 74, 1602–1613.
<https://doi.org/10.1093/icesjms/fsx016>
- Guthery, F.S., Burnham, K.P., Anderson, D.R., 2003. Model selection and multimodel Inference: a practical information-theoretic approach. *J. Wildl. Manage.*
<https://doi.org/10.2307/3802723>
- Hanselman, D.H., Heifetz, J., Echave, K.B., Dressel, S.C., Jech, J.M., 2015. Move it or lose it: movement and mortality of sablefish tagged in Alaska. *Can. J. Fish. Aquat. Sci.* 72, 238–251. <https://doi.org/10.1139/cjfas-2014-0251>
- Hanselman, D.H., Lunsford, C.R., Rodgveller, C.J., 2017. Assessment of the sablefish stock in Alaska in 2017. *Natl. Mar. Fish. Serv. Auke Bay Mar. Stn. 11305 Glacier Highw. Juneau, AK 99801* 576–717.
- Hilborn, R., Minte-Vera, C. V., 2008. Fisheries-induced changes in growth rates in marine fisheries: Are they significant?, in: *Bulletin of Marine Science.*
- Jasonowicz, A.J., Goetz, F.W., Goetz, G.W., Nichols, K.M., 2017. Love the one you're with: genomic evidence of panmixia in the sablefish (*Anoplopoma fimbria*). *Can. J. Fish. Aquat. Sci.* 74, 377–387. <https://doi.org/10.1139/cjfas-2016-0012>
- Johnson, K.F., Rudd, M.B., Pons, M., Akselrud, C.A., Lee, Q., Haltuch, M.A., Hamel, O.S., 2015. Status of the U.S. sablefish resource in 2015. http://www.pcouncil.org/wp-content/uploads/2015/05/D8_Att8_Sablefish_2015_Update_FULL-E-

[Only JUN2015BB.pdf](#)

- Kim, H.J., Miller, A.J., McGowan, J., Carter, M.L., 2009. Coastal phytoplankton blooms in the Southern California Bight. *Prog. Oceanogr.* 82, 137–147.
<https://doi.org/10.1016/j.pocean.2009.05.002>
- King, J.R., McFarlane, G.A., Beamish, R.J., 2001. Incorporating the dynamics of marine systems into the stock assessment and management of sablefish. *Prog. Oceanogr.* 49, 619–639.
[https://doi.org/10.1016/S0079-6611\(01\)00044-1](https://doi.org/10.1016/S0079-6611(01)00044-1)
- Kristensen, K., Nielsen, A., Berg, C., Skaug, H., Bell, B., 2016. TMB: Automatic Differentiation and Laplace Approximation. *Journal Stat. Softw.* 70, 1–21.
<https://doi.org/10.18637/jss.v070.i05>
- Mackas, D.L., Thomson, R.E., Galbraith, M., 2011. Changes in the zooplankton community of the British Columbia continental margin, 1985–1999, and their covariation with oceanographic conditions. *Can. J. Fish. Aquat. Sci.* 58, 685–702.
<https://doi.org/10.1139/f01-009>
- Mason, J.C., Beamish, R.J., McFarlane, G.A., 1983. Sexual maturity, fecundity, spawning, and early life history of sablefish (*Anoplopoma fimbria*) off the Pacific coast of Canada. *Can. J. Fish. Aquat. Sci.* <https://doi.org/10.1139/f83-247>
- McDevitt, M., 1990. Growth analysis of sablefish from mark-recapture data from the northeast Pacific. University of Washington.
- McGarvey, R., Fowler, A.J., 2002. Seasonal growth of King George whiting (*Sillaginodes punctata*) estimated from length-at-age samples of the legal-size harvest. *Fish. Bull.* 100, 545–558.
- Northwest Fisheries Science Center, 2019. West coast groundfish bottom trawl survey data - annual west coast time series groundfish trawl data collection survey from 2010-06-15 to 2010-08-15. <https://catalog.data.gov/dataset/west-coast-groundfish-bottom-trawl-survey-data-annual-west-coast-time-series-groundfish-trawl-d>
- Pacific Fisheries Management Council (PFMC), 2013. Pacific Coast fishery ecosystem plan for the U.S. portion of the California current large marine ecosystem. Pacific Fish. Manag. Counc. 7700 NE Ambassador Place, Suite 101, Portland, Oregon, 97220.
http://www.pcouncil.org/wp-content/uploads/FEP_FINAL.pdf
- Pörtner, H.O., Knust, R., 2007. Climate change affects marine fishes through the oxygen limitation of thermal tolerance. *Science* (80-.). <https://doi.org/10.1126/science.1135471>
- R Development Core Team, 2016. R: A Language and Environment for Statistical Computing. R Found. Stat. Comput. <https://doi.org/10.1007/978-3-540-74686-7>
- Rodionov, S.N., 2004. A sequential algorithm for testing climate regime shifts. *Geophys. Res. Lett.* 31, 2–5. <https://doi.org/10.1029/2004GL019448>
- Rutecki, L., Rodgveller, C.J., Lunsford, C.R., 2016. National Marine Fisheries Service longline survey data report and survey history, 1990–2014. 17109 Lena Point Loop Road Juneau, AK 99801. <https://doi.org/10.7289/V5/TM-AFSC-324>
- Schnute, J., 2008. A versatile growth model with statistically stable parameters. *Can. J. Fish. Aquat. Sci.* 38, 1128–1140. <https://doi.org/10.1139/f81-153>
- Shotwell, S.K., Hanselman, D.H., Belkin, I.M., 2014. Toward biophysical synergy: Investigating advection along the Polar Front to identify factors influencing Alaska sablefish recruitment. *Deep. Res. Part II* 107, 40–53. <https://doi.org/10.1016/j.dsr2.2012.08.024>
- Siddon, E., Zador, S., 2018. Ecosystem Status Report 2018: Eastern Bering Sea. North Pacific Fish. Manag. Counc. 605 W. 4th Ave. Suite 306 Anchorage, AK 99301.

- Simpson, G.L., 2018. Modelling palaeoecological time series using generalized additive models. bioRxiv. <https://doi.org/10.1101/322248>
- Stawitz, C.C., Essington, T.E., Branch, T.A., Haltuch, M.A., Hollowed, A.B., Spencer, P.D., 2015. A state-space approach for detecting growth variation and application to North Pacific groundfish. *Can. J. Fish. Aquat. Sci.* 72, 1316–1328. <https://doi.org/10.1139/cjfas-2014-0558>
- Taylor, B.M., Brandl, S.J., Kapur, M., Robbins, W.D., Johnson, G., Huveneers, C., Renaud, P., Choat, J.H., 2018. Bottom-up processes mediated by social systems drive demographic traits of coral-reef fishes. *Ecology* 99, 642–651. <https://doi.org/10.1002/ecy.2127>
- Thorson, J.T., 2019. Guidance for decisions using the Vector Autoregressive Spatio-Temporal (VAST) package in stock, ecosystem, habitat and climate assessments. *Fish. Res.* 210, 143–161. <https://doi.org/10.1016/j.fishres.2018.10.013>
- von Bertalanffy, L., 1957. Quantitative laws in metabolism and growth. *Q. Rev. Biol.* <https://doi.org/10.1086/401873>
- Waite, J.N., Mueter, F.J., 2013. Spatial and temporal variability of chlorophyll-a concentrations in the coastal Gulf of Alaska, 1998–2011, using cloud-free reconstructions of SeaWiFS and MODIS-Aqua data. *Prog. Oceanogr.* 116, 179–192. <https://doi.org/10.1016/j.pocean.2013.07.006>
- Wickham, H., Francois, R., Henry, L., Muller, K., 2019. dplyr: A Grammar of Data Manipulation.
- Williams, A.J., Farley, J.H., Hoyle, S.D., Davies, C.R., Nicol, S.J., 2012. Spatial and sex-specific variation in growth of albacore tuna (*Thunnus alalunga*) across the South Pacific Ocean. *PLoS One* 7. <https://doi.org/10.1371/journal.pone.0039318>
- Winton, M. V., Wuenschel, M.J., McBride, R.S., 2014. Investigating spatial variation and temperature effects on maturity of female winter flounder (*Pseudopleuronectes americanus*) using generalized additive models. *Can. J. Fish. Aquat. Sci.* <https://doi.org/10.1139/cjfas-2013-0617>
- Wood, S.N., 2011. Fast stable restricted maximum likelihood and marginal likelihood estimation of semiparametric generalized linear models. *J. R. Stat. Soc. Ser. B Stat. Methodol.* <https://doi.org/10.1111/j.1467-9868.2010.00749.x>
- Wood, S.N., 2003. Thin plate regression splines. *J. R. Stat. Soc. Ser. B Stat. Methodol.* <https://doi.org/10.1111/1467-9868.00374>
- Wyeth, M.R., Kronlund, A.R., Elfert, M., 2005. Summary of the 2005 British Columbia Sablefish (*Anoplopoma fimbria*) research and assessment survey: Canadian technical report of fisheries and aquatic sciences. Science Branch, Pacific Region Pacific Biological Station, Nanaimo, British Columbia V9T 6N7. http://publications.gc.ca/site/archivee Archived.html?url=http://publications.gc.ca/collections/collection_2012/mpo-dfo/Fs97-6-2694-eng.pdf